Electromagnetic modeling of parametric instability for slow waves in lower hybrid frequency range

J. Bao[1,2,a)], Z. Lin[3], W. L. Zhang[1,2,4] and D. Li[1,2,4]

[1]*Beijing National Laboratory for Condensed Matter Physics and CAS Key Laboratory of Soft Matter Physics, Institute of Physics, Chinese Academy of Sciences, Beijing 100190 China*
[2]*Univerisity of Chinese Academy of Sciences, Beijing 100049, China*
[3]*University of California, Irvine, CA 92697, USA*
[4]*Songshan Lake Materials Laboratory, Dongguan, Guangdong, 523808, China*

[a)]Corresponding author: jbao@iphy.ac.cn

Abstract. Lower hybrid (LH) wave has been widely used for non-inductive current drive in modern tokamak experiments with high power injection. LH parametric instability (PI) has been observed in many LH experiments and considered as the most likely candidate which causes the decrease of LH current drive efficiency. Traditional LH PI theories are mostly based on the electrostatic model given the fact that the slow wave branch in LH frequency range is a quasi-electrostatic wave. However, electrostatic description is not accurate for the plasma parameters of scraped-off layer(SOL) region where LH PIs are observed in current fusion experiments. Thus, in this work, we include the electromagnetic correction for slow wave and build up the corresponding nonlinear dispersion relation of PI. The electromagnetic effects on two major decay channels, i.e., ion sound quasi-mode (ISQM) and ion cyclotron quasi-mode (ICQM) are discussed.

INTRODUCTION

Parametric instabilities(PIs) of lower hybrid(LH) wave have been observed in experiments [1], and the nonlinear effects are confirmed to play significant role to wave-plasma coupling, propagation, absorption and plasma confinement.

The nonlinear dispersion relation based on the electrostatic (ES) model for LH waves are widely used to analyze the parametric processes during the wave injection [2][3], however, the electromagnetic (EM) effects of LH waves can not be ignored in the edge of modern tokamak, especially in the scraped-off layer (SOL) where PIs are observed. Thus, in order to analyze the LH wave parametric processes accurately and comprehensively, the EM effects need to be taken into account in the nonlinear dispersion relation of LH waves. In this work, we derived a new EM nonlinear dispersion relation for LH PIs in the SOL region of tokamak. Using plasma and LH wave antenna parameter on EAST tokamak and comparing the results between ES and EM LH PI dispersion relations, we found that: 1. The parallel nonlinearity contributes to the growth rates of ion cyclotron quasi-mode decay (ICQM) and ion sound quasi-mode decay (ISQM) in both ES and EM PI models, especially for the cases of small scattering angle decay. 2. The EM effect modifies both the nonlinear coupling coefficient through parallel nonlinearity and linear polarizations of three waves (pump wave, low frequency wave and sideband wave), which decreases the growth rates of PI compared to the ES results.

Reduced electromagnetic model for slow wave

Since slow wave in lower hybrid frequency range (aka LH wave) is a quasi-electrostatic wave, a reduced EM model [4] is applied in this study by removing the compressional magnetic perturbation associated with fast wave(whistler wave).

The poisson's equation and Ampere's law are:

$$\nabla^2 \phi = -4\pi(Z_i \delta n_i + q_e \delta n_e), \tag{1}$$

and

$$\nabla^2 \delta A_z = -\frac{4\pi}{c}(Z_i n_{i0}\delta u_i + q_e n_{e0}\delta n_e) + \frac{1}{c}\frac{\partial}{\partial t}\left(\mathbf{b_0}\cdot\nabla\phi + \frac{1}{c}\frac{\partial\delta A_z}{\partial t}\right), \quad (2)$$

where ϕ and δA_z are the ES potential and parallel vector potential.

Electron species is described by using drift kinetic equation:

$$\frac{\partial F_e}{\partial t} + v_z\frac{\partial F_e}{\partial z} + \nabla_\perp\cdot(\mathbf{V_{e\perp}}F_e) + \dot{v}_z\frac{\partial F_e}{\partial v_z} = 0, \quad (3)$$

where $\mathbf{V_{e\perp}} = v_z\frac{\delta\mathbf{B_\perp}}{B_0} + \frac{c\mathbf{b_0}\times\nabla\phi}{B_0} + \frac{\partial\nabla\phi}{\partial t}\frac{e}{m_e\Omega_{ce}^2}$ and $\dot{v}_z = -\frac{q_e}{m_e}\left[\left(\mathbf{b_0}+\frac{\delta\mathbf{B_\perp}}{\mathbf{B_0}}\right)\cdot\nabla\phi + \frac{1}{c}\frac{\partial\delta A_z}{\partial t}\right]$.

Ion species is described by 6-dimensional Vlasov equation:

$$\frac{\partial F_i}{\partial t} + \dot{\mathbf{X_i}}\cdot\nabla F_i + \dot{\mathbf{V_i}}\cdot\frac{\partial F_i}{\partial\mathbf{V_i}} = 0, \quad (4)$$

where $\dot{\mathbf{X_i}} = \mathbf{V_i}$, $\dot{\mathbf{V_i}} = \frac{Z_i}{m_i}\left(\delta\mathbf{E} + \frac{1}{c}\mathbf{V_i}\times B_0\right)$, and $\delta\mathbf{E} = -\nabla\phi - 1/c(\partial\delta A_z/\partial t)\mathbf{b_0}$. For LH waves, the parallel inductive electric field $\partial\delta A_z/\partial t$ in the ion's equation of motion could be ignored.

Eqs. (1-4) form a closed system, and the correspondingly linear dispersion relation in uniform plasmas is:

$$1 + \underbrace{\frac{2\omega_{pi}^2}{k^2v_i^2}\left[1 + \xi_i\sum_l Z\left(\frac{\omega-l\Omega_{ci}}{k_z v_i}\right)I_l(b_i)e^{-b_i}\right]}_{X_i} + \underbrace{\frac{2\omega_{pe}^2}{k^2v_e^2}\left[1 + \xi_e Z(\xi_e)\left(1 - \frac{k_\perp^2 v_e^2}{2\Omega_{ce}^2}\right)\right] + \frac{2\omega_{pe}^2}{k^2v_e^2}\left[1 + \xi_e Z(\xi_e)\right]\frac{P}{n^2-P}}_{X_e} = 0, \quad (5)$$

where X_i and X_e are the ion and electron susceptibilities, $P = 1 + \frac{2\omega_{pe}^2}{k_z^2 v_e^2}[1 + \xi_e Z(\xi_e)]$, $\xi_i = \omega/k_z v_i$, $\xi_e = \omega/k_z v_e$, $v_i = \sqrt{2T_i/m_i}$, $v_e = \sqrt{2T_e/m_e}$, $n_z = ck_z/\omega$ and $n_\perp = ck_\perp/\omega$ are the parallel and perpendicular refractive indices. Here, we compare the linear dispersion relations of LH wave from reduced model (Eq. (5)), Stix's fully EM model [5] and electrostatic model [2] in Figure 1, where we use EAST SOL parameters [1], i.e., $n_z = 2.11$, $f_{LH} = 2.45GHz$, $T_e = 100eV$ and $B = 1.8T$. It can be seen that above reduced EM model accurately describes the slow LH wave dispersion relation.
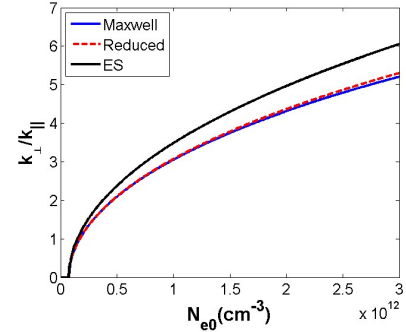

FIGURE 1. The comparison of slow LH wave linear dispersion relations between ES model [2], reduced EM model (Eq. (5)) and Stix fully EM model [5].

Nonlinear dispersion relation

In order to delineate the EM LH PI dispersion relation in a concise manner, we utilize fluid approach for the derivation of nonlinear coupling in this article, and kinetic approach will be reported systematically in a future publication. We use ω and $\mathbf{k}$ to represent wave frequency and wave vector for pump wave $(\omega_0, \mathbf{k_0})$, sideband wave $(\omega_1, \mathbf{k_1})$ and low frequency wave $(\omega, \mathbf{k})$, which satisfy the 3-wave coupling relations $\omega = \omega_0 + \omega_1$ and $\mathbf{k} = \mathbf{k_0} + \mathbf{k_1}$. Here, it should be noted that the sign of ω_1 is opposite to ω_0 and $|\omega_1| < |\omega_0|$, which represents the lower sideband wave.

The electron fluid velocities for pump wave, sideband wave and low frequency wave are $\mathbf{U_\perp^L} = -\frac{ie\phi}{m_e\Omega_{ce}}\mathbf{b_0}\times\mathbf{k_\perp}$ and $U_z^L = -\frac{iek_z}{m_e\omega}(\phi - \frac{\omega}{ck_z}\delta A_z)$, where $\Omega_{ce} = q_e B_0/cm_e$ is the electron cyclotron frequency, and k_z and $\mathbf{k_\perp}$ are the parallel and perpendicular wave vectors. The polarization drift is dropped due to the fact that wave frequency is much smaller than electron cyclotron frequency. Linearizing Eq. (3) and combining Eq. (2), the linearized relation between ES potential and parallel vector potential is $\delta A_z = \frac{n_z P}{P-n^2}\phi$. Please note that we omit the subscripts for different waves in fluid velocity equations.

The parallel ponderomotive force for the low frequency wave is $F_{pz} = -\frac{m_e}{2}(\mathbf{U_{0\perp}^L}\cdot\nabla U_{1z}^L + \mathbf{U_{1\perp}^L}\cdot\nabla U_{0z}^L + U_{0z}^L\mathbf{b_0}\cdot\nabla U_{1z}^L + U_{1z}^L\mathbf{b_0}\cdot\nabla U_{0z}^L) + \frac{q_e}{2c}(\mathbf{U_{0\perp}^L}\times\delta\mathbf{B_{1\perp}} + \mathbf{U_{1\perp}^L}\times\delta\mathbf{B_{0\perp}})$, where $\delta\mathbf{B_{0,1}} = \nabla\delta A_{0z,1z}\times\mathbf{b_0}$.

By defining the ponderomotive potential $F_{pz} = -q_e\mathbf{b_0} \cdot \nabla\phi_p$, we can obtain the low frequency ponderomotive potential as:

$$\phi_p = \frac{F_{pz}}{iek_z} = -\frac{ie\mathbf{k_{1\perp}} \cdot \mathbf{b_0} \times \mathbf{k_{0\perp}}}{2m_e\Omega_{ce}k_z}\frac{\omega_0 k_{1z} - \omega_1 k_{0z}}{\omega_0\omega_1}\phi_0\phi_1 - \frac{ek_{0z}k_{1z}}{2m_e\omega_0\omega_1}\left(1 + \underbrace{\frac{P_0}{n_0^2 - P_0}}_{\{I\}}\right)\left(1 + \underbrace{\frac{P_1}{n_1^2 - P_1}}_{\{II\}}\right)\phi_0\phi_1, \qquad (6)$$

where $n_0 = ck_0/\omega_0$, $n_1 = ck_1/\omega_1$ and $n = ck/\omega$ are the refractive indices for pump, sideband and low frequency waves, and P_0, P_1 and P are the elements of corresponding susceptibility. Terms $\{I\}$ and $\{II\}$ in Eq. (6) are the electromagnetic effects on ponderomotive force compared to the former electrostatic result [2, 3], where the parallel nonlinearity is corrected. In the ES limit, i.e., $n_0^2 \gg P_0$ and $n_1^2 \gg P_1$, Eq. (6) reduce to the well-known ES form [2, 3]. Note that the ponderomotive potential ϕ_p contains both nonlinear ES potential and nonlinear parallel vector potential contributions as $\phi_p = \phi^{NL} - (1/c)(\omega/k_z)\delta A_z^{NL}$. Thus, only giving ϕ_p in $\dot{v}_z$ and remove the third term in Eq. (3), the nonlinear electron density perturbation at low frequency is $\delta n_e^{NL} = \chi_e \frac{k^2}{4\pi e}\phi_p$, where $\chi_e = \frac{2\omega_{pe}^2}{k^2 v_e^2}[1 + \xi_e Z(\xi_e)]$ is the susceptibility of electron species with respect to ponderomotive potential ϕ_p, and the plasma function Z is kept here for the thermal effect of low frequency wave.

Substituting linear and nonlinear electron density perturbations into the Poisson's equation, the nonlinear equation for low frequency wave is $\Lambda\phi = -\frac{4\pi e}{k^2}\delta n_e^{NL}$, where $\Lambda = 1 + X_i + X_e$, X_i and X_e are defined by Eq. (5) for low frequency wave.

The nonlinear density perturbation of sideband wave satisfies the continuity equation: $\frac{\partial \delta n_{1e}^{NL}}{\partial t} + \frac{1}{2}\left(\delta n_e^L + \delta n_e^{NL}\right)\nabla \cdot \mathbf{U_0^{L*}} = 0$, where $*$ means the conjugate of complex number, δn_e^L is the linear electron density perturbation integrated from linearized Eq. (3) at low frequency, δn_e^{NL} is nonlinear electron density perturbation, and $\mathbf{U_0^{L*}}$ is the linear electron fluid velocity at pump wave frequency. Thus, the nonlinear equation of sideband wave can be obtained as $\Lambda_1\phi_1 = -\frac{4\pi e}{k_1^2}\delta n_{1e}^{NL}$, where $\Lambda_1 = 1 + X_{1i} + X_{1e}$, X_{1i} and X_{1e} are defined by Eq. (5) for sideband wave. (The subscript "1" should be added to ω_1, k_1, ξ_{i1}, ξ_{e1}, n_1 and P_1 in Eq. (5).)

Coupling nonlinear equations of low frequency wave and sideband wave together, we can readily get the nonlinear dispersion relation for EM slow wave:

$$\Lambda\Lambda_1 = M, \qquad (7)$$

where the nonlinear coupling coefficient $M = \frac{X_e - \Lambda}{X_e + \frac{\omega_{pe}^2}{\Omega_{ce}^2}\xi_e Z(\xi_e)}\frac{\omega_{pi}^2}{\omega_0^2}\frac{\omega_{pi}^2}{4k^2 c_s^2}[1 + \xi_e Z(\xi_e)]^2 \sin^2\delta_1\frac{u^2}{c_s^2}\left(1 + \eta_\parallel^2\right)\left(1 + \frac{P}{n^2 - P}\right)$, and $\eta_\parallel^2 = \frac{k_{0z}^2 k_{1z}^2 \Omega_{ce}^2}{\omega_0^2 k_{0\perp}^2 k_{1\perp}^2 \sin^2\delta_1}\left(1 + \frac{P_1}{n_1^2 - P_1}\right)\left(1 + \frac{P_0}{n_0^2 - P_0}\right)^2$ represents the parallel nonlinearity contribution. $c_s = \sqrt{T_e/m_i}$, δ_1 is the angle between pump and sideband waves, and $u = ck_{0\perp}|\phi_0|/B_0$ is the amplitude of $E \times B$ motion at pump wave frequency.

Electromagnetic effects on non-resonant decays

In this section, we solve Eq. (7) analytically for ISQM and ICQM decays, which are two major decay channels observed in experiments [1]. For non-resonant decay, the low frequency mode suffers strong Landau damping with $\Lambda(\omega_r, \mathbf{k}) \neq 0$, while sideband wave frequency is in LH frequency range, which is a propagating wave with $\Lambda_1(\omega_{1r}, \mathbf{k_1}) \approx 0$. Thus, the growth rate γ_p of PI can be derived by expanding Eq. (7) as $\gamma_p = -\gamma_{1L} + \frac{1}{\partial\Lambda_1/\partial\omega_{1r}}Im\left(\frac{M}{\Lambda}\right)$, where γ_{1L} and ω_{1r} are the linear Landau damping rate and the real frequency of sideband wave. Considering $\omega_r \approx kc_s$ for ISQM and $\omega_r - \Omega_{ci} \approx k_z v_i$ for ICQM, the PI growth rate dependences on density and scattering angle δ_1 are given in Figures 2 and 3. The dashed lines are the results from PI models without parallel nonlinearity, i.e., set $\eta_\parallel = 0$ in Eq. (7), and the solid lines are the results with finite $\eta_\parallel$ in Eq. (7). The black lines represent the results with applying ES approximation $n^2 \gg P$ (i.e., $\frac{P}{n^2 - P} = 0$) in Eq. (7)(i.e., the ES model used in previous LH PI studies [2][3]).

The parallel nonlinearities increase the growth rates of both ISQM and ICQM from both ES and EM PI models. Compared to ES results, it is seen that EM effect stablizes the LH PIs by modifying the linear dielectric constants of all three waves (pump wave, low frequency wave and sideband wave) and nonlinear coupling coefficient through parallel nonlinearity. It is also noted that the EM effects cause much weaker effect on the ExB component of coupling coefficient compared to the parallel component in Eq. (7). The mechanism of EM stabilization of PIs can be understood
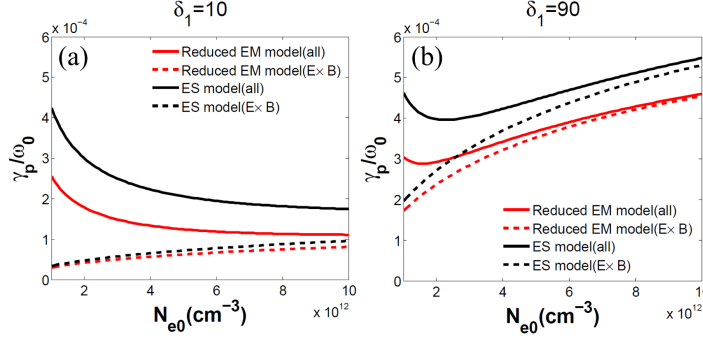
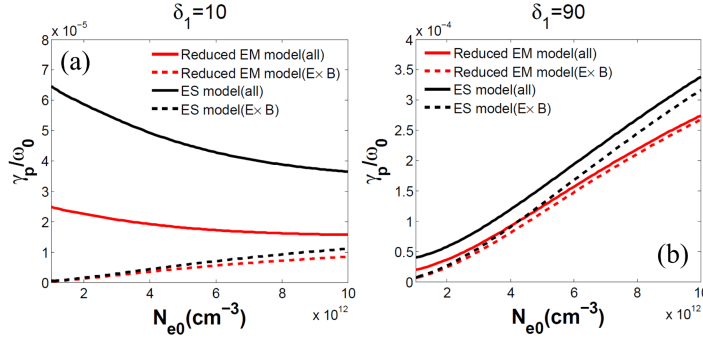**FIGURE 2.** The comparison of ISQM PI growth rate between ES model [2][3] and reduced EM model for (a) small scattering angle $\delta_1 = 10°$ and (b) large scattering angle $\delta_1 = 90°$. The dashed lines represent the results when $\eta_\parallel = 0$ in Eq. (7).

FIGURE 3. The comparison of ICQM PI growth rate between ES model [2][3] and reduced EM model for (a) small scattering angle $\delta_1 = 10°$ and (b) large scattering angle $\delta_1 = 90°$. The dashed lines represent the results when $\eta_\parallel = 0$ in Eq. (7).

as follows: the electrostatic approximation assumes that light speed is infinity compared to the wave phase velocity, which magnifies the plasma susceptibility, i.e., the wave electric fields give rise to larger plasma density perturbations compared to electromagnetic model with taking into account the finite ratio of light speed and wave phase velocity. In electromagnetic model, the smaller plasma susceptibility leads to the smaller density perturbations by pump wave and sideband wave, which nonlinearly form a weaker ponderomotive force and decrease the growth rates of PIs.

REFERENCES

[1] B. J. Ding, P. T. Bonoli, A. Tuccillo, *et al.*, Nucl. Fusion **58**, p. 095003 (2018).
[2] C. S. Liu and V. K. Tripath, Physics Reports **130**, 143–216 (1986).
[3] A. H. Zhao and Z. Gao, Nucl. Fusion **53**, p. 083015 (2013).
[4] Y. Lin, X. Y. Wang, L. Chen, and Z. Lin, Plasma Phys. Control. Fusion **47**, p. 657 (2005).
[5] T. Stix, *Waves in Plasmas* (American Institute of Physics, New York, 1992).